BMC Biology

RESEARCH

Open Access

# Functional genomics reveals key gene families and molecular pathways for extreme cold survival in the khapra beetle

Lingyu Zeng[1,2], Shiqian Feng[3], Sizhu Zheng[4], Göran Arnqvist[5], Yan Zhao[1,6], Shaokun Guo[1], Zihua Zhao[1] and Zhihong Li[1*]

## Abstract

**Background** The khapra beetle (*Trogoderma granarium* Everts) is among the world's most destructive invasive pests, threatening food security and international trade. Its larvae exhibit exceptional resilience to extreme cold, enabling expansion beyond typical habitats. However, the molecular mechanisms underlying its cold tolerance remain largely unexplored due to limited genomic resources.

**Results** We generated the first chromosome-level genome assembly for *T. granarium* (327 Mb, contig N50 = 883 kb), identifying 19,112 protein-coding genes across 9 chromosomes (99.0% BUSCO completeness). Comparative genomics revealed significant expansions in gene families associated with stress response, detoxification, and metabolism, including P450s, HSPs, and the insulin/IGF/relaxin family. Transcriptomic analysis and RNA interference targeting *INSR*, *PIK3CB*, and *ADCY9* demonstrated marked effects on mortality and development following cold exposure. Crucially, functional validation revealed distinct survival roles: while *INSR* and *PIK3CB* are essential for sustaining basal homeostasis under stress, *ADCY9* specifically mediates the response to cold adaptation. Additionally, miRNAs such as tca-miR-305-3p suggest post-transcriptional regulation of cold-responsive genes within the longevity and insulin signaling pathways.

**Conclusions** This study elucidates the genetic basis of *T. granarium*'s resilience, uncovering an integrated survival strategy involving both robust metabolic maintenance and targeted adaptive responses. These findings provide high-quality genomic resources and identify actionable molecular targets for the development of quarantine measures and invasion prevention strategies.

**Keywords** *Trogoderma granarium* Everts, Chromosome-level genome assembly, Cold tolerance, Invasion ability, Pest genomics

*Correspondence:
Zhihong Li
lizh@cau.edu.cn
Full list of author information is available at the end of the article

## Background

The khapra beetle, *Trogoderma granarium* Everts (Coleoptera: Dermestidae), is one of the 100 worst invasive species in the world and has been listed as a quarantine pest in many countries [1, 2]. The name "khapra" reflects the species' notorious persistence and destructive nature [3]. Khapra beetle larvae are ravenous feeders with a broad host range, including both plant and animal products [2]. They can completely devastate stored food supplies, causing up to 75% economic losses (Additional file 1: Fig. S1a and b) [4]. The beetle's exceptional tolerance to harsh environments and superior diapause ability enable it to rapidly invade and establish in new habitats [3, 5] posing severe threats to food security and international trade [6–8].

The khapra beetle is primarily distributed between 35° north (N) and 35° south (S), but was also been reported in higher latitude regions with colder climates, such as Norway (62° N), Russia (60° N), Denmark (56° N), and Ireland (53° N) (Additional file 1: Fig. S1c) [9]. Ambient temperature is a critical factor limiting the geographic distribution of insects [10]. Deviations from their thermal range can disrupt enzyme activity, cellular homeostasis, and metabolic rates, ultimately impairing survival and development [11]. Thus, the ability to withstand temperature stress is essential for successful colonization of new habitats. Despite eradication efforts in many regions, historical distribution records demonstrate the khapra beetle's resilience and adaptability to diverse environmental conditions. In recent years, interceptions of khapra beetles at quarantine ports have increased steadily in countries such as China, the USA, and Australia [3]. Given its invasive potential, many countries not infested remain at risk of importing the beetle through international trade. Understanding the mechanisms underlying its remarkable cold tolerance is therefore of critical economic and quarantine importance.

As ectothermic organisms, insects exhibit phenotypic plasticity in response to variable temperatures [12], enabling them to cope with environmental changes over short- or medium-term periods [13]. This plasticity can manifest as morphological alterations, life history modifications, and differential gene expression [14]. However, research on the khapra beetle has been limited, partly due to a lack of biological and genomic resources. High-quality genome assemblies can provide insights into species-specific gene families associated with stress resistance, such as heat shock proteins (HSPs), cytochrome P450 monooxygenases (P450s), and insulin/IGF/relaxin families [15–17]. Without an annotated genome, however, comparative genomic and functional studies are hindered, leaving our understanding of the beetle's cold tolerance largely confined to ecological and physiological experiments [3, 18]. Furthermore, while evidence suggests that microRNAs (miRNAs) may promote survival at low temperatures through unique regulatory mechanisms [19, 20], their role in Dermestidae beetles remains unexplored.

In this study, we de novo generated the first chromosome-level genome of the khapra beetle and conducted comparative evolutionary analyses with other resilient insect species. Using transcriptomic and functional approaches, we investigated the effects of low temperature on survival and development in its laboratory populations, identifying key signaling pathways and genes involved in the response. Additionally, we employed small RNA sequencing and bioinformatics to predict miRNAs potentially associated with cold temperature. Our study aims to elucidate the genetic mechanisms underlying the khapra beetle's remarkable cold tolerance and to provide novel resources for developing effective strategies to prevent infestation and control this invasive pest.

## Results

### A chromosome-level genome assembly for the khapra beetle

We assembled and annotated a high-quality chromosome-level genome of the khapra beetle by combining Illumina, PacBio, and Hi-C sequencing with transcriptome data. Initially, we generated 21.2 Gb of Illumina raw-read data (70,675,373 paired reads, ~ 50 × coverage), and a 21-mer genome survey predicted a genome size of 278 Mb with relatively high duplication (1.58%) and heterozygosity (1.24%) (Additional file 1: Fig. S2). We further produced 35.7 Gb of PacBio long-read data (~ 126 × coverage) with a subread N50 of 28.4 kb and an average read length of 24.2 kb. Following redundancy purging and correction, we obtained a 327 Mb draft genome comprising 1116 contigs with a contig N50 of 913 kb (Additional file 1: Table 1). This draft was then scaffolded with 26.4 Gb of Hi-C sequencing data (88,026,344 read pairs), of which 82.7% were uniquely aligned. After manual curation, we successfully assembled a final chromosome-level genome with a total size of 327 Mb and a scaffold N50 of 38 Mb. This assembly consists of 9 major chromosomes (Fig. 1a and b), covering 93.97% of the draft genome with a contig N50 of 883 kb (Additional file 1: Table 1). Benchmarking Universal Single-Copy Orthologs (BUSCO) analysis indicated high completeness (Fig. 1c), with the draft genome reaching 99.1% (90.9% single-copy, 8.2% duplicated, 0.5% missing), and the chromosome-level assembly reaching 99.0% (96.3% single-copy, 2.7% duplicated, 0.5% missing).

For annotation, we constructed a TruseqmRNA-seq (Eukaryotes) library and generated 11.0 Gb of

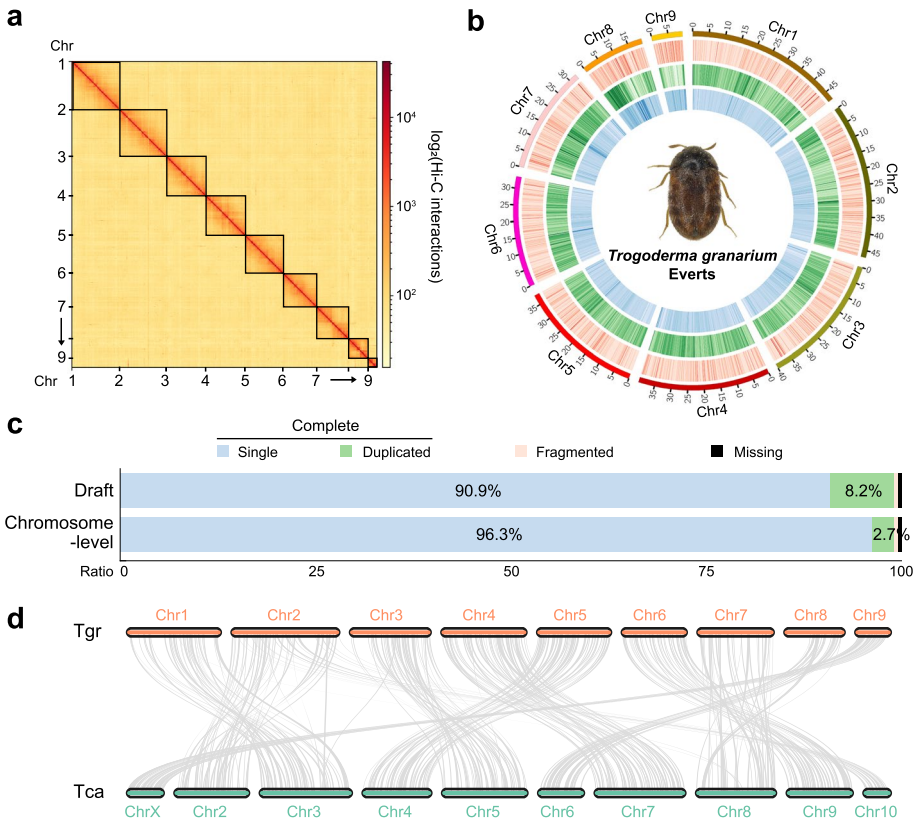


**Fig. 1** Chromosome-level genome architecture of the khapra beetle. **a** Hi-C contact heatmap showing genome-wide chromosomal interactions. **b** Circos plot of the nine chromosomes (outer tracks) displaying gene density (red), repeat content (green), and GC content (blue). **c** Genome completeness assessment using BUSCO. **d** Whole-genome synteny comparison between the khapra beetle (Tgr) and *Tribolium castaneum* (Tca)

full-length transcriptome data. Structural annotation identified 154 Mb of 625,392 repeat elements, occupying 47.13% of the genome (Additional file 1: Table 2), including DNA transposon (12.4%), retrotransposons such as long interspersed nuclear elements (LINEs, 16.87%) and long terminal repeats (LTRs, 17.86%), and other repeat motifs. We also identified 1678 non-coding RNAs (Additional file 1: Table 3) and 19,112 protein-coding genes with a mean length of 8403 bp (Additional file 1: Table 4). Functional annotation assigned potential roles to 16,969 genes, of which the majority were successfully annotated in multiple databases, including NR (88.65%), Swiss-Prot (58.29%), KEGG (37.01%), GO (29.40%), and eggNOG (84.50%) (Additional file 1: Fig. S3, Additional file 1: Table 5). The completeness of the protein-coding gene set was further evaluated using BUSCO, which identified 98.6% of the conserved orthologs (Additional file 1: Table 5), confirming the high quality of our gene models. Together, these results provide a comprehensive, high-quality genome assembly and annotation for the khapra beetle (Fig. 1b).

## Conserved synteny and evolutionary divergence among beetles

We first investigated synteny between the khapra beetle (Tgr) and *Tribolium castaneum* (Tca), the main model species among beetles (Fig. 1d). These analyses revealed that a large segment of Chr9 in the khapra beetle is collinear with a corresponding region of *T. castaneum* ChrX, indicating that Chr9 represents the X chromosome of the khapra beetle, a conclusion further supported by the presence of conserved X-linked markers on this chromosome, such as *G6PD*, *MSL2*, and *MSL3*. In addition, we identified two fission events: khapra beetle Chr2 represents a fusion of segments derived from *T. castaneum* Chr2 and Chr10, while Chr8 of *T. granarium* incorporates sequences from *T. castaneum* Chr6 and Chr8. Despite these rearrangements, gene order within homologous segments of the two species remains largely conserved, with most differences attributable to a limited number of fission events in the khapra beetle genome.

To place the khapra beetle in a broader evolutionary context, we conducted a comparative genomic analysis involving 18 species: ten globally recognized invasive pests (including *T. granarium*) and eight non-invasive

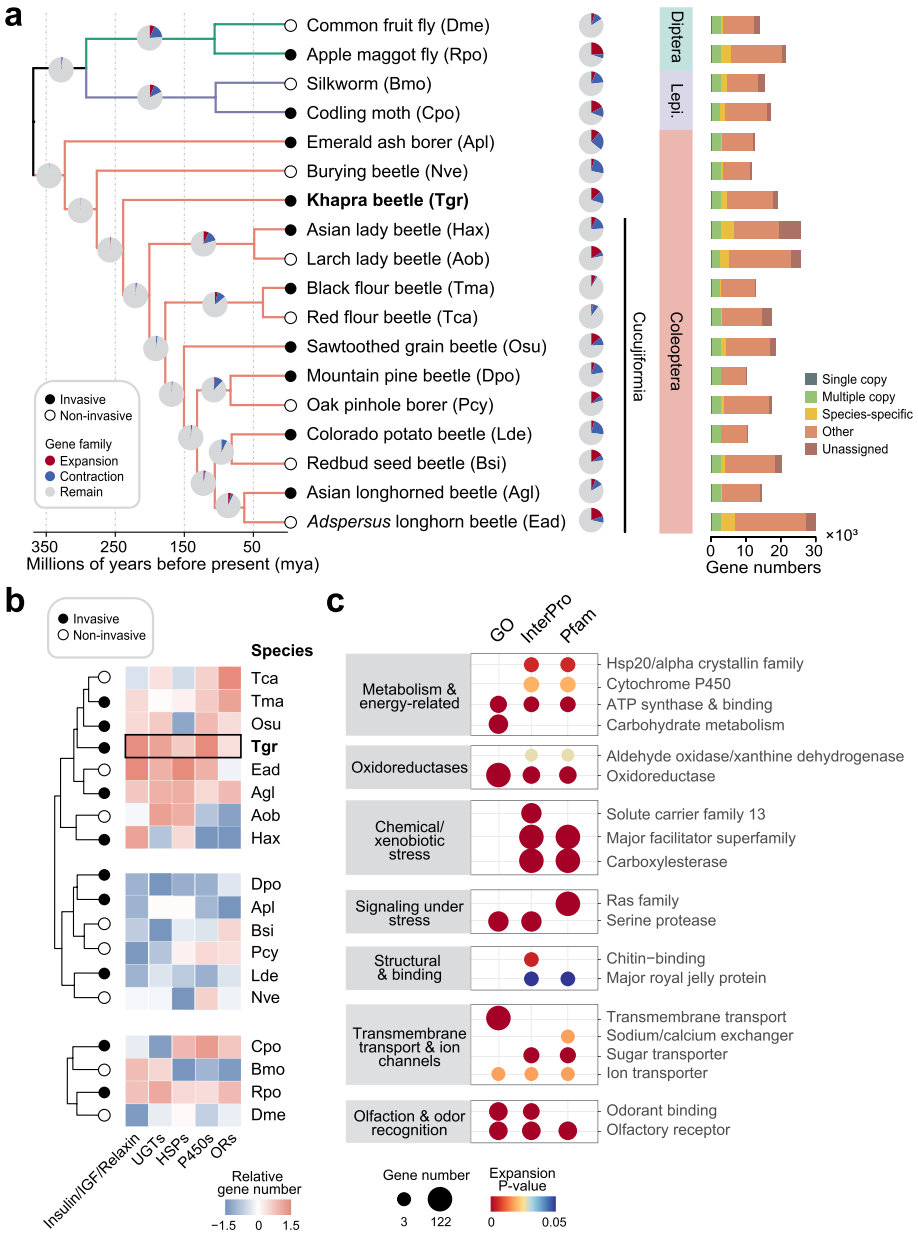


**Fig. 2** Comparative genome evolution and functional expansion in the khapra beetle. **a** Phylogenomic relationships and gene family dynamics across selected insect species. **b** Abundance of representative gene families in beetles based on BITACORA v1.3 annotations. Relative gene counts within each family were scaled separately for beetles and outgroups due to high gene numbers in Cpo and Rpo. **c** Functional annotation of significantly expanded gene families ($p < 0.05$) in the khapra beetle identified by CAFE v5 and KinFin v1.0

controls (Fig. 2a, Additional file 1: Table 6). Using OrthoFinder v2.5.1, we clustered 286,650 genes (91.4% of the total) into 21,943 orthogroups (Additional file 1: Table 7). Among these, 2639 orthogroups were shared across all species, including 319 composed entirely of single-copy genes. For *T. granarium*, 1919 of its 19,112 genes were assigned to 413 species-specific orthogroups (Additional file 1: Table 8). Tandem sequences of single-copy genes generated were then used to reconstruct the species phylogeny. The resulting tree resolved Coleopteran, Lepidopteran, and Dipteran species into three distinct clades. Using MCMCTREE, we estimated that *T. granarium* diverged from Cucujiformia beetles approximately 240 million years ago (mya) (Fig. 2a), consistent with the calibration range of 225–250 mya applied in our analysis.

### Expansion of stress resistance-related gene families

The khapra beetle is highly polyphagous, remarkably tolerant to harsh environmental conditions, and exhibits a well-developed diapause capability, enabling it to adapt to and colonize new environments [3, 5] and infest a wide range of stored agricultural products [6–8]. To investigate the potential genomic basis of these adaptive traits, we first analyzed the overall evolution of gene families across the selected species. Comparative analysis revealed that gene family expansions were largely lineage-specific rather than strictly correlated with invasiveness (Fig. 2a and b), and the khapra beetle (Tgr) stood out with a substantial proportion of expanded gene families. Notably, relative to other Coleopteran species, *T. granarium* displayed remarkable expansions in the insulin/IGF/relaxin family, which is essential for growth and development, as well as in the UDP-glucuronosyl transferases (UGTs) and P450s families, which are key to pesticide resistance and detoxification (Fig. 2b, Additional file 1: Tables 9 and 10).

Among the 1305 expanded gene families identified in the khapra beetle, functional annotation based on GO terms, InterPro, and Pfam databases revealed significant enrichment ($p < 0.05$) in pathways critical for survival. These included metabolism and energy production (e.g., ATPase families), stress response and protein folding (e.g., HSP20/α-crystallin), and xenobiotic detoxification (e.g., P450s, solute carriers, and carboxylesterases). We also observed expansions in families regulating stress signaling (e.g., Ras and serine proteases), transmembrane transport (e.g., sugar transporters), and chemosensation (olfaction and odor recognition) (Fig. 2c, Additional file 2: Table 11). Collectively, these expanded gene families likely provide the genomic basis for the khapra beetle's exceptional stress tolerance and capacity to colonize diverse and challenging habitats.

### Survival and gene expression under cold stress

To explore how the khapra beetle utilizes its stress-related genomic repertoire to withstand low temperatures, we examined its physiological performance and transcriptional responses under cold exposure (Fig. 3a). Larvae were subjected to a low-temperature treatment (−1°C), which imposed significant thermal stress (Additional file 1: Fig. S4a and b). After 5 days, larval development was markedly impaired, with survival (86.50 ± 4.54%), pupation rate (31.00 ± 12.32%), pupal period (5.55 ± 0.50 d), and pupal weight (1.54 ± 0.63 mg) all significantly reduced compared to controls (Additional file 1: Fig. S4c–f).

Using the chromosome-level genome assembly as a reference, we identified 4408 differentially expressed genes (DEGs) in response to cold stress ($|\log_2\text{FoldChange}| > 1$, $p_{adj} < 0.05$), including 2621 upregulated and 1787 downregulated genes (Fig. 3b and c, Additional file 2: Table 12). To establish a link between genomic evolution and cold tolerance, we intersected these DEGs with the genes from significantly expanded gene families ($p < 0.05$). This analysis identified 335 overlapping genes (Additional file 2: Table 12), which were significantly enriched in pathways critical for cold tolerance (Fig. 3d), such as energy metabolism (protein processing, cholesterol metabolism, steroid biosynthesis, and fatty acid biosynthesis), stress signaling (MAPK and AMPK signaling pathways), and regulatory processes (insulin signaling and longevity-regulating pathways). Consistent with these findings, broader GO enrichment of all upregulated genes (149 terms) revealed activation of pathways related to lipid storage, the stress-activated MAPK cascade, and responses to heat (Additional file 1: Fig. S5a, Additional file 2: Table 13), while downregulated genes (250 terms) were associated with nutrient response and amino acid metabolism (Additional file 1: Fig. S5b, Additional file 2: Table 14). Furthermore, KEGG pathway analysis of the total DEGs identified 32 significantly enriched pathways ($p_{adj} < 0.05$, $q < 0.05$) (Additional file 2: Table 15), with 26 pathways (e.g., oxidative phosphorylation, thermogenesis, and longevity-regulating pathways) showing high significance ($p_{adj} < 0.01$, $q < 0.01$) (Additional file 1: Fig. S5c). Several genes involved in the longevity-regulating and insulin signaling pathways were notably upregulated (Fig. 3e and f), including insulin-like peptide receptor (*INSR*, Chr05_g11712), phosphatidylinositol-4,5-bisphosphate 3-kinase catalytic subunit (*PIK3CB*, Chr06_g13868), adenylate cyclase type 9 (*ADCY9*, Chr05_g10254), cAMP-dependent protein kinase catalytic subunit (*PRKACA*, Chr03_g06686), ribosomal protein S6 kinase alpha-5 (*RPS6KA5*, Chr01_g02000), superoxide dismutase (*SOD2*, Chr07_g14199), and catalase-rel domain containing protein (*CAT*, Chr02_g04085). These findings indicate that the khapra beetle enhances metabolic flexibility, energy homeostasis, and oxidative stress defense to maintain cellular function under cold stress, thereby supporting its capacity to survive and establish in colder environments.

### Verification of gene function under cold stress

Quantitative real-time reverse transcription PCR (qRT-PCR) tests confirmed that the expression of *INSR*, *PIK3CB*, *ADCY9*, *PRKACA*, and *RPS6KA5* was significantly upregulated under low-temperature conditions, showing fold increase of 1.73, 3.05, 4.68, 5.36, and 12.96, respectively (Fig. 3f). In contrast, the expression levels of *SOD2* and *CAT* remained unchanged compared to the control, suggesting that upstream genes in the longevity-regulating pathway may contribute to cold stress

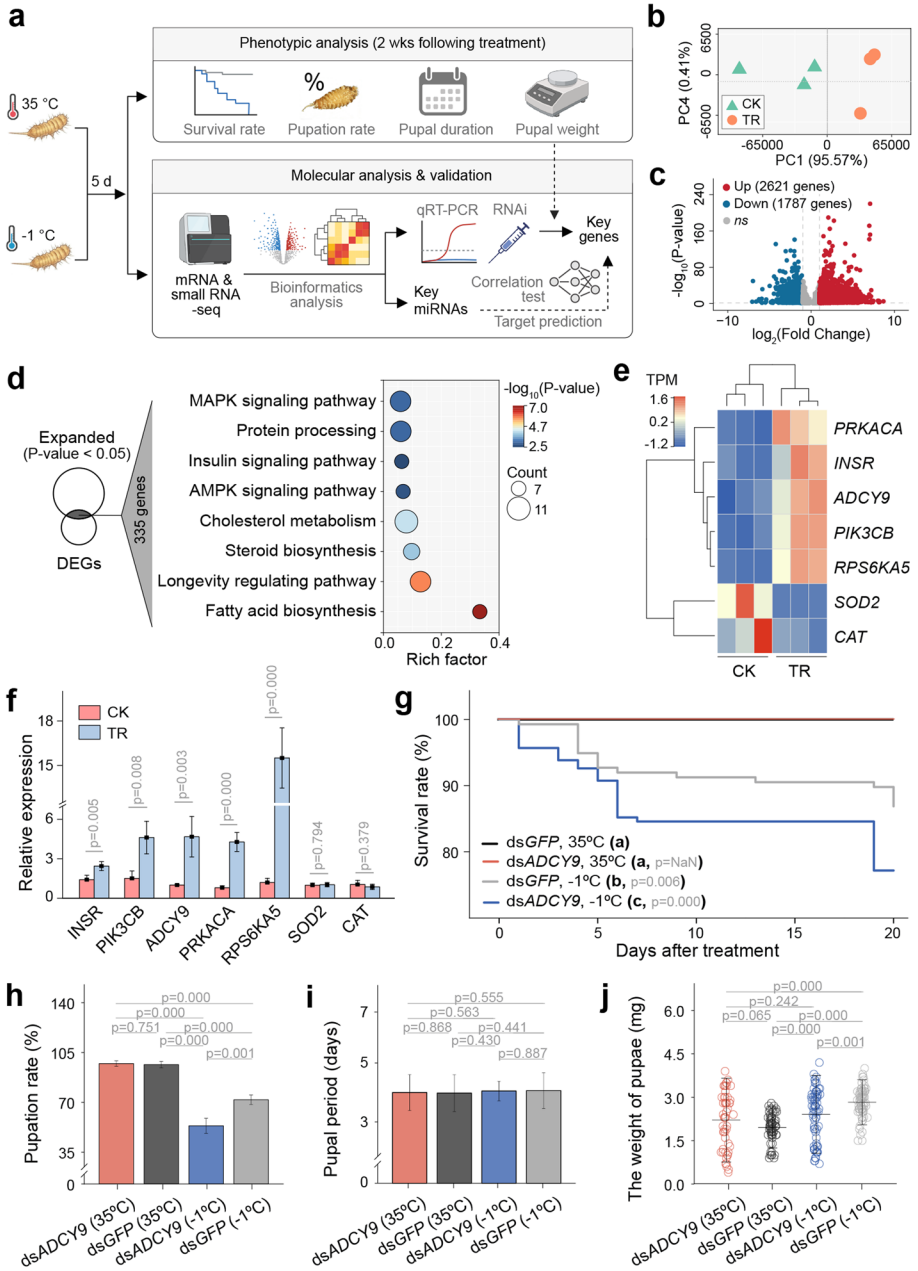


**Fig. 3** Transcriptomic analysis and functional validation of cold tolerance mechanisms in the khapra beetle. **a** Schematic workflow for analyzing cold tolerance mechanisms. **b** Principal component analysis of cold-treated (TR) versus control (CK) samples. **c** Volcano plot of differentially expressed genes (DEGs) ($|\log_2\text{FoldChange}| > 1$, $p_{adj} < 0.05$). **d** KEGG pathway enrichment analysis of the overlapping genes between significantly expanded gene families ($p < 0.05$) and DEGs ($p_{adj} < 0.01$, $q < 0.01$). **e** Heatmap of DEGs involved in the longevity-regulating pathway. **f** qRT-PCR validation of selected genes under cold stress. Functional effects of *ADCY9* RNAi under cold stress: relative daily survival (**g**), pupation rate (**h**), pupal duration (**i**), and pupal weight (**j**)

adaptation. To validate the functional roles of these upregulated genes, we performed RNAi knockdown in late fourth-instar larvae. Prior to functional assays, we optimized the double-stranded RNA (dsRNA) dosage using a concentration gradient (34, 75, and 150 ng), identifying 75 ng as the most effective dosage for achieving maximal silencing (Additional file 1: Fig. S6a). Using this optimized dosage (75 ng), all target genes exhibited significantly reduced transcript levels 3 days post-injection (Additional file 1: Fig. S6b–f). Under cold stress, larvae treated with ds*INSR*, ds*PIK3CB*, and ds*ADCY9* exhibited significantly reduced survival rates (11.39 ± 5.9%,

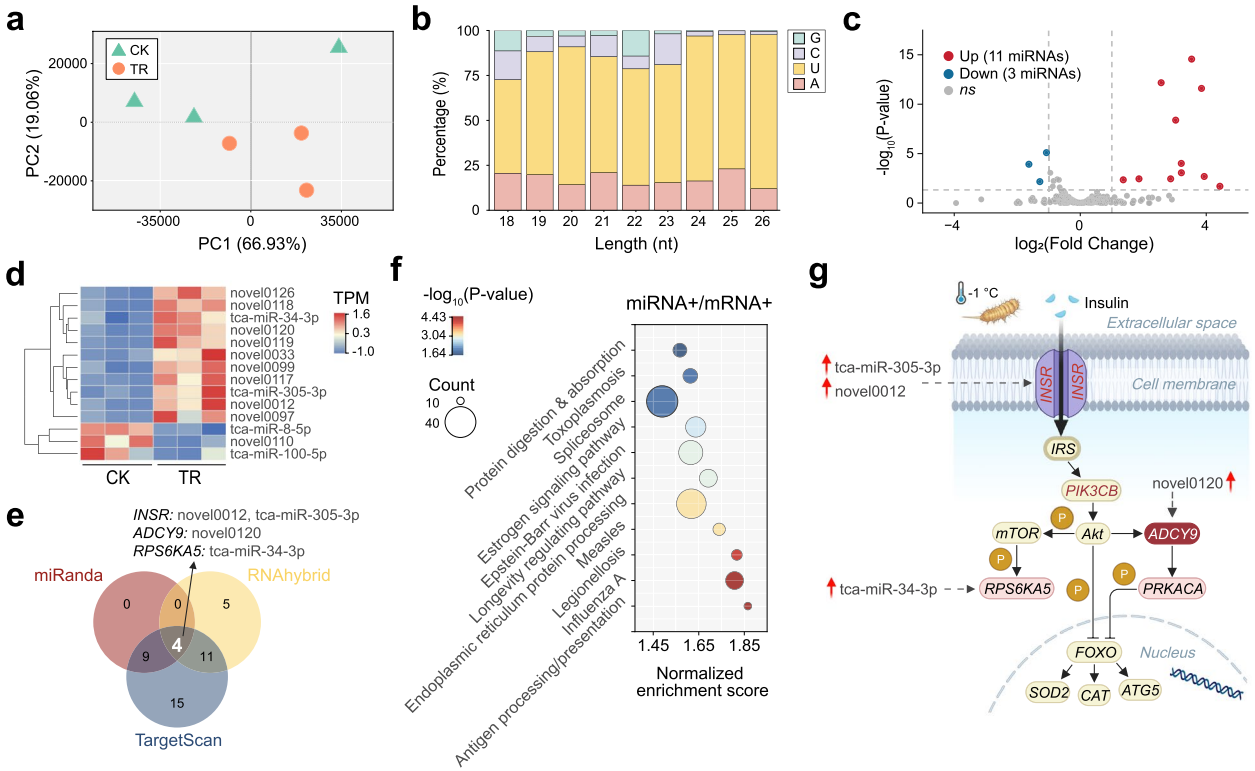


**Fig. 4** Putative miRNA regulatory networks underlying cold tolerance in the khapra beetle. **a** Principal component analysis of miRNA profiles under cold stress (TR) and control (CK) conditions. **b** First nucleotide bias distribution of known and novel miRNAs across different sequence lengths. **c** Volcano plot of differentially expressed miRNAs (DEMs) ($|\log_2\text{FoldChange}| > 1$, $p_{adj} < 0.05$). **d** Heatmap illustrating hierarchical clustering of significant DEMs. **e** Venn diagram showing the prediction of miRNA targets within the longevity-regulating pathway using miRanda v3.3a, RNAhybrid v2.1.2, and TargetScan. **f** Joint KEGG pathway enrichment of upregulated DEMs and their target genes (miRNA + /mRNA +) ($p_{adj} < 0.05$, $q < 0.05$). **g** Schematic of the putative regulatory network involving insulin signaling and longevity pathways under cold stress. Genes verified by RNAi to significantly impact cold survival or development are highlighted in red (red box: *ADCY9*; red font: *INSR*, *PIK3CB*). Dashed arrows indicate predicted miRNA-target interactions

69.84 ± 7.04%, and 73.42 ± 4.47%, respectively) compared to the ds*GFP* (dsRNA of green fluorescent protein) control group (Fig. 3g, Additional file 1: Fig. S7a, c). To distinguish between general developmental defects and specific cold-tolerance impairment, we also monitored phenotypes at the control temperature (35°C). Notably, knockdown of *INSR* and *PIK3CB* resulted in high lethality and failed pupation at both cold and control temperatures (Additional file 1: Fig. S7b). This indicates that these upstream signaling components are essential for basal survival and development. Their significant upregulation under cold stress (Fig. 3f) suggests that robust signaling activity of these essential components is required to withstand the metabolic demands of cold stress. In contrast, *ADCY9* knockdown showed a distinct genotype-by-environment interaction. The fitness consequences, including mortality and impaired pupal development, were significantly more severe under cold conditions than at 35°C (Fig. 3h–j), highlighting a specific role for *ADCY9* in enhancing cold tolerance.

### Differential expression of miRNAs associated with the longevity-regulating pathway under cold stress

To further explore post-transcriptional regulation under cold exposure, we constructed small RNA libraries using the same samples employed for transcriptome sequencing (Fig. 4a, Additional file 1: Table 16). The majority of small RNAs ranged from 18 to 26 nt, with a dominant peak at 22 nt, and the first nucleotide at the 5′ end showed a strong preference for uracil (70.27%) (Fig. 4b, Additional file 1: Tables 17 and 18). Using miRDeep2, we identified 235 miRNAs, including 123 novel candidates and 112 conserved miRNAs previously reported in *T. castaneum*. Among them, 14 miRNAs were differentially expressed in response to cold stress ($|\log_2\text{FoldChange}| > 1$, $p_{adj} < 0.05$), with 11 being upregulated and 3 being downregulated (Fig. 4c and d, Additional file 1: Table 19). These differentially expressed miRNAs were predicted to target 6736 genes, and their expression levels were significantly correlated with those of target transcripts ($|r| > 0.4$) (Additional file 2: Table 20).

Within the longevity-regulating pathway, we identified high-confidence miRNA-target pairs by intersecting predictions from three independent computational algorithms (miRanda, RNAhybrid, and TargetScan) (Fig. 4e). Functional enrichment analyses of these robustly predicted and positively correlated miRNA-mRNA pairs revealed significant overrepresentation of GO terms related to the MAPK cascade, stress-activated protein kinase signaling, and regulation of cellular response to stress, as well as enrichment of the longevity-regulating pathway in KEGG analysis (Fig. 4f, Additional file 1: Figs. S8 and S9). In the resulting putative regulatory network (Fig. 4g), *INSR* was predicted to be targeted by tca-miR-305-3p and novel0012, while *ADCY9* and *RPS6KA5* showed potential interactions with novel0120 and tca-miR-34-3p, respectively (Additional file 2: Table 20). These findings suggest that miRNAs responding to low temperature may contribute to the fine-tuning of insulin-related and longevity-associated signaling pathways. The observed positive correlations hint at a complex post-transcriptional regulatory mechanism consistent with the transcriptional activation of these genes in the mRNA dataset.

## Discussion

High-quality genomic resources are essential for understanding the mechanisms underlying invasiveness and environmental adaptation in insects [21, 22]. As a globally significant quarantine pest, the khapra beetle (*Trogoderma granarium* Everts) poses major biosafety and economic threats, particularly to stored agricultural products [1–4]. The chromosome-level genome presented here provides a robust framework for molecular investigations, enabling comparative, evolutionary, and functional studies.

The assembled genome (327 Mb) was slightly larger than the k-mer estimate (278 Mb), likely reflecting residual heterozygosity (1.24%) and duplicate sequences (1.58%) (Additional file 1: Fig. S2) [23]. Repetitive elements, particularly DNA transposons, often correlate with genome size [24–26], and they accounted for 47.13% and 12.40% of the genome, respectively (Additional file 1: Table 2), which may complicate assembly. Although multiple generations of inbreeding can reduce heterozygosity [15], this approach is impractical for khapra beetles. We therefore combined long-read, Hi-C, and transcriptomic data to generate a near-complete, highly contiguous genome (Fig. 1a and b, Additional file 1: Table 1) [27–29]. Notably, our Hi-C data resolved the genome into nine chromosomal scaffolds, which is highly congruent with the known cytogenetic profile of the genus *Trogoderma* (typically 2n = 18), as documented in historical karyotype surveys [30]. This convergence between physical chromatin interaction mapping and classical evolutionary evidence provides strong confidence in the chromosomal architecture of our assembly. This high-quality resource, further validated by BUSCO analyses (99.0% completeness, Fig. 1c), now enables accurate gene annotation and functional inference for stress-related gene families and pathways.

Despite diverging ~ 250 million years ago, the khapra beetle and *T. castaneum* show high synteny, with limited fission events (Fig. 1d). This remarkable collinearity underscores strong conservation of gene order across Coleopterans and provides confidence in the assembly's structural accuracy. Specifically, the khapra beetle Chr9 aligns with *T. castaneum* ChrX, indicating its identity as the X chromosome (Fig. 1d). Phylogenomic analyses further confirmed divergence times and evolutionary relationships in agreement with previous studies (Fig. 2a), placing the khapra beetle in the broader context of resilient insect species [31].

Gene family expansions likely underpin the beetle's adaptability and invasiveness. Our comparative analysis revealed significant expansions in detoxification (P450s, UGTs, carboxylesterases), stress response (HSPs), olfaction-related gene families, and metabolism (insulin/IGF/relaxin) (Fig. 2b and c, Additional file 1: Table 9, Additional file 2: Table 11). The expansion of detoxification-related genes aligns with the beetle's documented resistance to malathion, methyl bromide, and phosphine [3, 32, 33], whereas expanded HSPs likely contribute to thermal tolerance, starvation resilience, and general stress response [34]. Likewise, expansions in odorant-binding proteins and odorant receptors may enhance host detection, feeding plasticity, and oviposition site selection [28]. The insulin/IGF/relaxin gene family, which involves insulin, insulin-like growth factors, and relaxin family peptides (including insulin-like peptides) [35], plays a crucial role in the regulation of growth and development, metabolism, fertility, stress resistance, and longevity [36]. Together, these genomic adaptations provide a molecular explanation for the beetle's invasiveness, and targeting these gene families with RNA-based biopesticides may offer novel pest-control strategies, although ecological efficacy requires further evaluation.

Temperature is a major factor limiting insect distribution, and the khapra beetle's survival in high-latitude regions suggests exceptional cold tolerance [9, 10]. Its most cold-tolerant stage is old larva, where > 90% mortality is only achieved under −10°C for 30 days [18]. Our experiments confirmed that low-temperature exposure (−1°C) significantly reduced larval survival, pupation rate, pupal period, and pupal weight (Additional file 1: Fig. S4), validating the phenotypic impact of cold stress. Transcriptomic analyses identified differential expression

of genes in lipid metabolism, MAPK signaling, oxidative phosphorylation, and thermogenesis (Additional file 1: Fig. S5, Additional file 2: Table 13). Importantly, we identified 335 genes at the intersection of expanded gene families and cold-responsive DEGs (Fig. 3d), with significant enrichment in the insulin signaling and longevity-regulating pathways. This finding reveals an evolutionary basis for the beetle's physiological response and provides a strong rationale for our subsequent focus on key genes within these pathways. Notably, our functional analysis highlights how different layers of the insulin signaling pathway coordinate to support survival under cold stress. First, *INSR* and *PIK3CB* were identified as fundamental components essential for basal survival, as their knockdown caused high lethality even at control temperatures (Additional file 1: Fig. S7). However, their significant upregulation under cold stress suggests that maintaining robust signaling activity through these core components is a prerequisite for the organism to withstand environmental stress (Fig. 3f). Studies have shown that insulin-like peptides and their pathways regulate substance and energy metabolism in response to changes in external environments in insects, as demonstrated by effects on tissue and organ development as well as on size and body weight [37]. Activation of *INSR* and *PIK3CB* is key for regulating anabolism, cell growth, and metabolic processes [37, 38]. Under cold stress, the demand for these homeostatic processes likely increases, requiring elevated expression of these upstream genes to prevent physiological collapse.

Beyond these general metabolic roles, definitive evidence has linked the insulin/insulin-like growth factor signaling (IIS) pathway specifically to insect cold tolerance. For example, in *Drosophila melanogaster*, the IIS system co-regulates cold-resistant behaviors, such as food acquisition under thermal stress [39]. Furthermore, in the mosquito *Culex pipiens*, the IIS pathway is a master regulator of the overwintering response and associated stress tolerance [40]. In *T. granarium*, the significant expansion and cold-induced upregulation of this pathway suggest that it has been evolutionary co-opted to meet the extreme metabolic demands of its highly resilient larvae. In contrast, *ADCY9* exhibited a more specific role in cold adaptation. Its knockdown resulted in significantly more severe mortality and developmental impairment under cold conditions compared to the control temperature (Fig. 3). *ADCY9* can act as integrators of transmembrane signal transduction [41], and our results suggest it is specifically recruited to modulate signaling intensity in response to low temperatures. Together, these findings demonstrate that cold adaptation in *T. granarium* relies on a dual mechanism: the reinforcement of essential basal pathways (*INSR*, *PIK3CB*) to maintain viability and the recruitment of stress-specific modulators (*ADCY9*) to fine-tune energy homeostasis and defense responses.

Post-transcriptional regulation by miRNAs appears to be another layer of the cold adaptation mechanism. Using a stringent intersection approach with three independent algorithms, we identified high-confidence miRNA-target pairs, such as tca-miR-305-3p and novel0120, which showed significant positive correlations with key genes in the insulin and longevity pathways (Fig. 4, Additional file 1: Table 19, Additional file 2: Table 20). Evidence from other insect species supports the biological relevance of these findings. The differential expression of miR-8-3p under low temperature mirrors patterns observed in overwintering individuals of the rice water weevil, *Lissorhoptrus oryzophilus* [42]. Similarly, a functional link between miR-305 and the insulin signaling pathway has been demonstrated in the oriental fruit fly, *Bactrocera dorsalis* [43], where the miR-305 loss disrupts energy metabolism. Notably, while miRNAs are typically associated with mRNA repression [44, 45], we observed a positive correlation between miR-305 and its predicted targets, consistent with findings in *B. dorsalis* [43]. This suggests a complex regulatory scenario, potentially involving indirect regulation or feedback loops that maintain homeostasis under stress, although the precise molecular mechanisms await experimental validation.

Based on the conserved insulin signaling pathway in *D. melanogaster* [46] and our computational predictions, we propose a putative mechanistic model for cold tolerance in the khapra beetle (Fig. 4g). In this hypothetical network: Cold stress induces the upregulation of *INSR*, which is predicted to be targeted by tca-miR-305-3p and novel0012. Concurrently, *PIK3CB*, potentially modulated by novel0120, may facilitate signal transduction to *ADCY9* [47]. In parallel, tca-miR-34-3p shows a strong correlation with *RPS6KA5* (*MSK1*), a kinase known to phosphorylate transcription factors like CREB [48]. Collectively, while direct biochemical verification is needed, the robustness of these multi-algorithm predictions suggests that these miRNA-mRNA interactions likely constitute a fine-tuning mechanism. This network would enhance metabolic activity and protein translation, thereby contributing to the khapra beetle's resilience against low temperatures.

## Conclusions

We present the first chromosome-level genome of *Trogoderma granarium* and integrate transcriptomic and functional analyses to uncover the genetic basis of its remarkable cold tolerance and invasiveness. Key expansions in detoxification, stress-response, metabolic, and olfactory gene families, together with insulin and longevity pathway regulation by both mRNAs

and miRNAs, underpin the beetle's ability to survive low temperatures and colonize diverse habitats. Functional validation revealed that cold survival relies on an integrated signaling mechanism: the reinforcement of essential upstream components (*INSR* and *PIK3CB*) to sustain basal homeostasis, combined with the specific action of adaptive modulators (*ADCY9*) to enhance cold tolerance. These findings provide foundational insights into the molecular mechanisms driving invasiveness, offering broadly relevant resources for understanding adaptation and resilience in other invasive insect species.

## Methods

### Insect strains

The *Trogoderma granarium* population used in this study was originally intercepted from an Iranian cargo ship in May 2013. Beetles were subsequently reared on peanut meal in an artificial climatic chamber at 35 ± 1°C and 65% relative humidity in constant darkness [49]. To prevent escape, all work involving live insects was conducted under strict containment conditions at Suzhou Customs District. The developmental duration of young larvae (first to fourth instars) and old larvae (fifth instar and older) was approximately 23 days and 7 ~ 8 days, respectively [50]. Preliminary observations indicated that larvae at 28 days post-hatching exhibited signs of imminent pupation (e.g., cessation of feeding, increased excretion, and movement to the food surface).

### Sampling, sequencing, and library construction for high-quality genome

Genomic DNA was extracted from 40 male pupae using the Wizard SV Genomic DNA Purification System (Promega, Madison, USA) for both Illumina (short-read) and PacBio (long-read) sequencing. For Hi-C library construction, an additional 40 male pupae were processed at Berry Genomics (Beijing, China), where chromatin was cross-linked with formaldehyde and digested with *MboI*, followed by random fragmentation into 300 ~ 500 bp fragments. For transcriptome data required for genome annotation, mixed samples representing different developmental stages (five eggs, three larvae, two pupae, and two adults) were collected, and total RNA was extracted using the RNAsimple Total RNA Kit (Tiangen, Beijing, China). All sequencing was performed at Berry Genomics (Beijing, China) using the Illumina NovaSeq platform (RRID:SCR_016387) and PacBio Sequel system (RRID:SCR_017990).

### Genome survey, draft assembly, and polishing

Genome size, heterozygosity, and repeat content were estimated using Jellyfish v2.2.1 (RRID:SCR_005491) ($k$ = 21) and GenomeScope v2.0 (RRID:SCR_017014) [27, 51]. PacBio reads were assembled using Canu v2.1.1 (RRID:SCR_015880) (minReadLength = 2000, minOverlapLength = 500, corOutCoverage = 120, corMinCoverage = 2) [52]. Long reads were mapped to the draft genome and error-corrected using pbmm2 v1.4.0 (https://github.com/PacificBiosciences/pbmm2) and gcpp v1.9.0 (https://github.com/PacificBiosciences/gcpp). Illumina reads were aligned to the corrected assembly using BWA v0.7.17 (RRID:SCR_010910) [53], and final polishing was performed with Pilon v1.23 (RRID:SCR_010910) [54].

### Chromosome-level genome assembly

The polished assembly was scaffolded using Juicer (RRID:SCR_017226) and 3D-DNA v180114 [55, 56], followed by manual curation in Juicebox v1.11.08 (RRID:SCR_021172) [57]. Genome completeness was evaluated using BUSCO v5.1.3 (RRID:SCR_015008) with the arthropoda_odb10 database [58]. Whole-genome synteny between *T. granarium* and the reference species *T. castaneum* was examined and visualized using jcvi [59].

### Genome annotation

Repeat sequences were identified de novo using RepeatModeler v2.0.1 and RepeatMasker v4.1.0 [60, 61]. Gene prediction integrated evidence from homologous Coleopteran genomes (*T. castaneum*, *Harmonia axyridis*, *Rhagonycha fulva*, *Propylea japonica*, and *Coccinella septempunctata*), ab initio predictions from SNAP (RRID:SCR_007936) and Augustus v3.0.3 (RRID:SCR_008417), and evidence integration by EVM (RRID:SCR_014659) [62–64]. Functional annotation was conducted by aligning protein sequences to the NCBI NR, Swiss-Prot, and eggNOG databases using DIAMOND (RRID:SCR_009457) [65]. GO terms and KEGG pathway information were assigned through Blast2GO (RRID:SCR_005828) and eggNOG-mapper v2.1.7 (RRID:SCR_021165) [66, 67].

### Ortholog identification, phylogeny, and divergence time estimation

Orthologous and paralogous genes were identified using OrthoFinder v2.5.1 (RRID:SCR_017118) (Additional file 1: Table 6) [68]. The dataset included ten globally recognized invasive pests (including *T. granarium*) selected from either the CABI Invasive Species Compendium (https://www.cabidigitallibrary.org/product/QI) or the

EPPO Global Database (https://www.eppo.int/ACTIVITIES/invasive_alien_plants/iap_lists), characterized by aggressive invasiveness and devastating agricultural impact. Eight related non-invasive species were included as controls to ensure that observed gene family changes primarily reflect adaptation to invasiveness rather than phylogenetic effects. Notably, while some species in the non-invasive group are significant pests (e.g., *Tribolium*), they were classified as non-invasive for this study because they do not meet the strict invasive or quarantine criteria defined by these international organizations. Phylogenetic trees were constructed with single-copy orthologs using RAxML [69]. Divergence times were estimated in MCMCTREE (PAML v4.9, RRID:SCR_014932) based on the calibration of 237 ~ 261 mya for *T. granarium* and Cucujiformia lineages (Fig. 2a) [70, 71].

#### Inference of gene family dynamic

To investigate gene family expansion and contraction, we utilized CAFE v5 (RRID:SCR_005983), modeling gene gain and loss rates across the phylogeny. The global parameter λ was estimated using a birth–death model to account for background genomic change. PAML v4.9 was applied to refine branch length estimations (parameters: rgene_gamma = 2, 18.75) [70, 72]. Families showing significant size changes were identified based on a $p$ value threshold of 0.05, with functional enrichment performed via KinFin v1.0 [73]. Furthermore, specific adaptive gene families—including those associated with insecticide resistance, sensory perception, and cold tolerance—were meticulously annotated using BITACORA v1.3. This workflow integrated HMM models from Pfam (http://pfam-legacy.xfam.org/) and high-quality NCBI protein datasets (critical $e$-value = 1e − 5) to mitigate annotation biases and capture lineage-specific expansions in *T. granarium* (Additional file 1: Table 10) [74].

#### Cold tolerance assays

Old larvae, previously reported as the most cold-tolerant [3, 18], was used for thermal tolerance experiments. To determine critical temperature thresholds, groups of 35 larvae were exposed to 35°C (control), 0°C, −1°C, −2°C, −3°C, −4°C, or −5°C for a duration of 7 days [75], then recovered under rearing conditions. Four biological replicates were included per treatment, and mortality was assessed after 2 weeks. Immobile, darkened larvae were recorded as dead [49].

To evaluate time-dependent physiological effects, larvae were exposed to −1°C or the control temperature (35°C) for durations of 1, 3, 5, or 7 days. These intervals were selected based on the 5 ~ 10-day window typically required to observe significant physiological shifts in insect cold hardiness. Following recovery, survival rates, pupation rate, pupal duration, and pupal weight were recorded to quantify the developmental impact of cold stress.

#### RNA sequencing and differential expression analysis

For transcriptome profiling, larvae exposed to −1°C or 35°C for 5 days followed by 1 h recovery were used. This 5-day time point was selected as it represented the earliest interval where significant developmental impairments were consistently observed in our preliminary assays. Each replicate ($n$ = 3) included five larvae. Total RNA was extracted using the RNAsimple kit (Tiangen, Beijing, China) and sequenced by Lianchuan Bio (Hangzhou, China). Low-quality reads and adapters were removed using fastp v0.23.2 (RRID:SCR_016962) [76]. Clean reads were aligned to the *T. granarium* genome, and gene counts were obtained using featureCounts v2.0.1 and analyzed by DESeq2 via the Trinity v2.11.0 pipeline [77].

#### qRT-PCR

cDNA synthesis was performed using the PrimeScript™ RT reagent kit with gDNA Eraser (TaKaRa, Kyoto, Japan), followed by 5 × dilution. qRT-PCR reactions were run using TranStart® Top Green qPCR SuperMix (+ Dye II) (TransGen, Beijing, China). Primer pairs (Additional file 1: Table 21) were designed with NCBI Primer-BLAST. *β-actin* (*ACTB*) was validated as a stable reference gene. Relative expression levels were calculated by the $2^{-\Delta\Delta Ct}$ method.

#### Gene cloning and RNA interference

Gene-specific primers were designed based on conserved protein domains identified through NCBI's CD-Search and appended with T7 promoter sequences (5′ -TAA TACGACTCACTATAGG-3′) at 5′ end (Additional file 1: Table 21). dsRNAs were synthesized using the T7 RiboMAX™ Express RNAi System (Promega, Madison, USA) and verified via NanoDrop ND-1000 and agarose electrophoresis.

For functional validation, groups of 35 late 4th-instar larvae were injected with 75 ng of dsRNA into the intersegmental membrane between the second and third to last abdominal segments using a DRUMMOND Nanoject II microinjector. To maintain consistent gene silencing, injections were repeated every 72 h, starting from the late 4th-instar stage and continuing until the larvae reached 28 days of age. This regimen ensured that each larva received at least two injections prior to the commencement of cold stress. Following the final injection at 28 days old, the larvae were subjected to cold stress (−1°C) for 5 days, followed by a 2-week recovery period under standard conditions (35°C). RNAi efficiency was assessed by qRT-PCR at 72 h post-injection. Larval

survival and developmental performance were monitored throughout the recovery period. ds*GFP* served as a control.

### Small RNA sequencing and analyses

The same RNA samples used for transcriptome sequencing were used for small RNA libraries by Lianchuan Bio Company (Hangzhou, Zhejiang, China). Clean reads (18 ~ 26 nt) were generated using fastp v0.23.2 [76] and TrimGalore v0.6.10 (-stringency 3, -phred33) (https://github.com/FelixKrueger/TrimGalore), de-duplicated with mapper.pl in miRDeep2 v0.1.3 [78]. Known miRNAs were annotated by aligning to miRBase (v22.1), Rfam (v15.5), and *T. granarium* genome features (allowing ≤ 2 mismatches). Novel miRNAs were predicted from unannotated reads using miRDeep2.pl (-r 5), with *T. castaneum* as the reference species.

### Differentially expressed miRNAs (DEMs) and interaction analysis

DEMs were identified from miRNA count data using miRDeep2's quantifier.pl script. Target genes were predicted using miRanda v3.3a (-en −10, -strict module), RNAhybrid v2.1.2 [79] (-b 10, -c, -f, 2&8, -m 10,000, -v 3, -u 3, -s 3utr_fly, -e −20), and TargetScan (http://www.targetscan.org) (default parameters). To ensure high confidence, only miRNA-target pairs independently predicted by the intersection of all three tools were retained for subsequent analysis. Pearson's correlation coefficients (PCCs) between miRNAs and mRNAs were calculated across all samples. Potential regulatory pairs were identified based on a correlation threshold of $|PCC| > 0.4$.

### Statistical analysis

All statistical analyses were performed in SPSS v25 (SPSS Inc., IL, USA). Welch's ANOVA and Games-Howell tests were used for multiple comparisons. Survival was analyzed by Cox proportional hazards models, with final survival rates compared using $\chi^2$ test when exceeding 50%. Pupation rate, pupal duration, pupal weight, and qRT-PCR results were analyzed by *t*-tests. Expression data were arcsine-transformed for correlation analysis using asin() and rcorr() functions in RStudio v1.4.1717 (RRID:SCR_000432) [80]. Statistical significance was defined as $p < 0.05$. Error bars were presented as mean values ± SD. Graphs were generated using iTOL (RRID:SCR_018174) (https://itol.embl.de/), Microsoft Office 2010 (RRID:SCR_016137), and Origin v2023b (OriginLab Corporation, MA, USA).

#### Abbreviations

| | |
|---|---|
| HSPs | Heat shock proteins |
| P450s | Cytochrome P450 monooxygenases |
| BUSCO | Benchmarking Universal Single-Copy Orthologs |
| Tgr | *Trogoderma granarium* |
| Tca | *Tribolium castaneum* |
| UGTs | UDP-glucuronosyl transferases |
| DEGs | Differentially expressed genes |
| *INSR* | Insulin-like peptide receptor |
| *PIK3CB* | Phosphatidylinositol-4,5-bisphosphate 3-kinase catalytic subunit |
| *ADCY9* | Adenylate cyclase type 9 |
| *PRKACA* | CAMP-dependent protein kinase catalytic subunit |
| *RPS6KA5* | Ribosomal protein S6 kinase alpha-5 |
| *SOD2* | Superoxide dismutase |
| *CAT* | Catalase-rel domain containing protein |
| dsRNA | Double-stranded RNA |
| ds*GFP* | Double-stranded RNA of green fluorescent protein |
| IIS | Insulin/insulin-like growth factor signaling |

## Supplementary Information

The online version contains supplementary material available at https://doi.org/10.1186/s12915-026-02551-5.

Additional file 1.

Additional file 2.

#### Acknowledgements

We are grateful to Shengfang Zhang, Guoping Zhan, Lijun Liu and Yujia Qin for technical advice.

#### Authors' contributions

L. Z. performed the experiments, analyzed the data, and wrote the manuscript. S. F. provided bioinformatics guidance. S. Z. and Z. Z. assisted with sample collection. Y. Z. and S. G. provided additional data analysis during the manuscript revision. Z. L. and G. A. were the major contributors to the manuscript revision. All authors read and approved the final manuscript.

#### Funding

This work was supported by the Joint Research Program of State Key Laboratory of Agricultural and Forestry Biosecurity (no. SKLJRP2509), the earmarked fund for China Agriculture Research System (CARS-02-32), the Teaching Team Program of China Agricultural University and the 2115 Talent Development Program of China Agricultural University, and the Swedish Research Council VR (no. 2019-03611).

#### Data availability

Raw sequencing data (Illumina DNA/RNA/miRNA, PacBio, and Hi-C) are available in the NCBI Sequence Read Archive (SRA) under BioProject PRJNA1032860. The genome assembly has been deposited under WGS accession JAWRCW000000000 (version JAWRCW010000000). The genome annotation file has been uploaded to https://doi.org/10.6084/m9.figshare.30784010. The 17 insect genome sequences utilized for comparative analysis in this study (Additional file 1: Table 6) were obtained from the NCBI database [reference [81–97] in the manuscript]. All data supporting this study are included within the article and its supplementary materials.

## Declarations

#### Ethics approval and consent to participate

Not applicable.

#### Consent for publication

Not applicable.

#### Competing interests

The authors declare no competing interests.

#### Author details

[1]State Key Laboratory of Agricultural and Forestry Biosecurity, MARA Key Laboratory of Surveillance and Management for Plant Quarantine Pests, College of Plant Protection, China Agricultural University, Beijing 100193, China. [2]MOE

Laboratory of Biosystems Homeostasis and Protection and Zhejiang Provincial Key Laboratory for Cancer Molecular Cell Biology, Life Sciences Institute, Zhejiang University, Hangzhou, Zhejiang, China. [3]State Key Laboratory for Biology of Plant Diseases and Insect Pests, Institute of Plant Protection, Chinese Academy of Agricultural Sciences, Beijing 100193, China. [4]Suzhou Customs District, Suzhou 215000, China. [5]Animal Ecology, Department of Ecology and Genetics, Evolutionary Biology Centre, Uppsala University, Uppsala 75236, Sweden. [6]State Key Laboratory of Agricultural and Forestry Biosecurity, Fujian Agriculture and Forestry University, Fuzhou 350002, China.

Received: 13 October 2025 Accepted: 11 February 2026
Published online: 23 February 2026

## References

1. Lowe SBM, Boudjelas S, De Poorter M. 100 of the world's worst invasive alien species: a selection from the global invasive species database. Invasive Species Specialist Group, World Conservation Union; 2000.
2. IPPC ISPM 27. Diagnostic protocols for regulated pests, DP 3: *Trogoderma granarium* Everts. 2016. https://www.ippc.int/static/media/files/publication/en/2016/01/DP_03_2012_En_2012-05-04_REV.pdf.
3. Athanassiou CG, Phillips TW, Wakil W. Biology and control of the khapra beetle, *Trogoderma granarium*, a major quarantine threat to global food security. Annu Rev Entomol. 2019;64:131–48.
4. Sudesh J, Kapoor AC. Effect of storage and insect infestation on protein and starch digestibility of cereal grains. Food Chem. 1992;44(3):209–12.
5. Zhang SF, Fan XH, Gao Y, Zhan GH. Beetles of stored products. China Science Publishing & Media Ltd; 2016.
6. Pasek JE. In: Khapra beetle (*Trogoderma granarium* Everts): pest-initiated pest risk assessment. Raleigh: USDA-APHIS; 1998.
7. Hagstrum DW, Subramanyam B. Stored-product insect resource. St. Paul, MN: AACC International; 2009.
8. Christos GA, Nickolas GK, Maria CB. Population growth of the khapra beetle, *Trogoderma granarium* Everts (Coleoptera: Dermestidae) on different commodities. J Stored Prod Res. 2016;69:72–7.
9. Athanassiou CG. *Trogoderma granarium* (khapra beetle). CABI https://www.cabidigitallibrary.org/doi/epdf/https://doi.org/10.1079/cabicompendium.55010 (2023).
10. Ma CS, Ma G, Pincebourde S. Survive a warming climate: insect responses to extreme high temperatures. Annu Rev Entomol. 2021;66:163–84.
11. Atkinson D. Temperature and organism size a biological law for ectotherms? Adv Ecol Res. 1994;25:1–58.
12. Bradshaw AD. Evolutionary significance of phenotypic plasticity in plants. Adv Genet. 1965;13:115–55.
13. Sgrò CM, Terblanche JS, Hoffmann AA. What can plasticity contribute to insect responses to climate change? Annu Rev Entomol. 2016;61:433–51.
14. Pavan F, Floreani C, Barro P, Zandigiacomo P, Montà L. Occurrence of two different development patterns in *Lobesia botrana* (Lepidoptera: Tortricidae) larvae during the second generation. Agric For Entomol. 2013;15(4):398–406.
15. Guo SK, Cao LJ, Song W, Shi P, Gao YF, Gong YJ, et al. Chromosome-level assembly of the melon thrips genome yields insights into evolution of a sap-sucking lifestyle and pesticide resistance. Mol Ecol Resour. 2020;20(4):1110–25.
16. Semaniuk U, Piskovatska V, Strilbytska O, Strutynska T, Burdyliuk N, Vaiserman A, et al. *Drosophila* insulin-like peptides: from expression to functions – a review. Entomol Exp et Appl. 2021;169(2):195–208.
17. Feng S, Opit G, Deng W, Stejskal V, Li Z. A chromosome-level genome of the booklouse, *Liposcelis brunnea*, provides insight into louse evolution and environmental stress adaptation. Gigascience. 2022. https://doi.org/10.1093/gigascience/giac062.
18. Wilches D, Laird R, Floate KD, Fields P. Effects of extreme temperatures on the survival of the quarantine stored-product pest, *Trogoderma granarium* (Khapra beetle). Proceedings of the 11th international working conference on stored product protection Chiang Mai, Thailand. 2014. https://opus.uleth.ca/server/api/core/bitstreams/f480eadd-11b9-4c30-b53d-36d8c85367b6/content.
19. Courteau LA, Storey KB, Morin P Jr. Differential expression of microRNA species in a freeze tolerant insect. Eurosta solidaginis Cryobiology. 2012;65(3):210–4.
20. Lyons PJ, Lang-Ouellette D, Morin P Jr. CryomiRs: towards the identification of a cold-associated family of microRNAs. Comp Biochem Physiol D Genomics Proteomics. 2013;8(4):358–64.
21. Hou L, Zhan S, Zhou X, Wang XH. Advances in research on insect genomics in China. Chin J Appl Entomol. 2017;54:693–704.
22. Huang C, Li YZ, Yang NW, Wu Q, Xing LS, Qian WQ, et al. Progresses in invasive insect genomics. Plant Prot. 2019;45(5):112–20.
23. Li F, Zhao X, Li M, He K, Huang C, Zhou Y, et al. Insect genomes: progress and challenges. Insect Mol Biol. 2019;28(6):739–58.
24. Blommaert J, Riss S, Hecox-Lea B, Mark Welch DB, Stelzer CP. Small, but surprisingly repetitive genomes: transposon expansion and not polyploidy has driven a doubling in genome size in a metazoan species complex. BMC Genomics. 2019;20(1):466.
25. Talla V, Suh A, Kalsoom F, Dinca V, Vila R, Friberg M, et al. Rapid increase in genome size as a consequence of transposable element hyperactivity in wood-white (Leptidea) butterflies. Genome Biol Evol. 2017;9(10):2491–505.
26. Kidwell MG. Transposable elements and the evolution of genome size in eukaryotes. Genetica. 2002;115(1):49–63.
27. Marçais G, Kingsford C. A fast, lock-free approach for efficient parallel counting of occurrences of k-mers. Bioinformatics. 2011;27(6):764–70.
28. Wan F, Yin C, Tang R, Chen M, Wu Q, Huang C, et al. A chromosome-level genome assembly of *Cydia pomonella* provides insights into chemical ecology and insecticide resistance. Nat Commun. 2019;10(1):4237.
29. Yin D, Ji C, Ma X, Li H, Zhang W, Li S, et al. Genome of an allotetraploid wild peanut *Arachis monticola*: a de novo assembly. Gigascience. 2018. https://doi.org/10.1093/gigascience/giy066.
30. Smith SG, Virkki N. Animal cytogenetics insecta 5. Berlin: Gebruder Borntraeger; 1978.
31. McKenna DD, Shin S, Ahrens D, Balke M, Beza-Beza C, Clarke DJ, et al. The evolution and genomic basis of beetle diversity. Proc Natl Acad Sci U S A. 2019;116(49):24729–37.
32. Heckel DG. Insect detoxification and sequestration strategies. In Annual Plant Reviews, eds Voelckel C and Jander G. 2014:77–114.
33. Simon JY. Encyclopedia of entomology. Dordrecht: Springer; 2004.
34. Ding JH, Zheng LX, Chu J, Liang XH, Wang J, Gao XW, et al. Characterization, and functional analysis of Hsp70 and Hsp90 gene families in Glyphodes pyloalis Walker (Lepidoptera: Pyralidae). Front Physiol. 2021;12:753914.
35. Blundell TL, Humbel RE. Hormone families: pancreatic hormones and homologous growth factors. Nature. 1980;287(5785):781–7.
36. Chowanski S, Walkowiak-Nowicka K, Winkiel M, Marciniak P, Urbanski A, Pacholska-Bogalska J. Insulin-like peptides and cross-talk with other factors in the regulation of insect metabolism. Front Physiol. 2021;12:701203.
37. Chen XA, Yao HW, Ye GY. Research advances on insulin-like peptides and their functions in insects. Chin J Biol Control. 2017;33:699–712.
38. Lin X, Yu N, Smagghe G. Insulin receptor regulates food intake through sulfakinin signaling in the red flour beetle, *Tribolium castaneum*. Peptides. 2016;80:89–95.
39. Lingo PR, Zhao Z, Shen P. Co-regulation of cold-resistant food acquisition by insulin- and neuropeptide Y-like systems in Drosophila melanogaster. Neuroscience. 2007;148(2):371–4.
40. Sim C, Denlinger DL. Insulin signaling and FOXO regulate the overwintering diapause of the mosquito Culex pipiens. Proc Natl Acad Sci U S A. 2008;105(18):6777–81.
41. Ishikawa Y, Homcy CJ. The adenylyl cyclases as integrators of transmembrane signal transduction. Circ Res. 1997;80(3):297–304.
42. Lewis BP, Shih IH, Jones-Rhoades MW, Bartel DP, Burge CB. Prediction of mammalian microRNA targets. Cell. 2003;115(7):787–98.
43. Xie J, Chen H, Zheng W, Cai Z, Li X, Zhang H. MiR-275/305 cluster is essential for maintaining energy metabolic homeostasis by the insulin signaling pathway in *Bactrocera dorsalis*. PLoS Genet. 2022;18(10):e1010418.
44. Lin CC, Chen YJ, Chen CY, Oyang YJ, Juan HF, Huang HC. Crosstalk between transcription factors and microRNAs in human protein interaction network. BMC Syst Biol. 2012;6:18.
45. Shriram V, Kumar V, Devarumath RM, Khare TS, Wani SH. MicroRNAs as potential targets for abiotic stress tolerance in plants. Front Plant Sci. 2016;7:817.
46. Miron M, Lasko P, Sonenberg N. Signaling from Akt to FRAP/TOR targets both 4E-BP and S6K in Drosophila melanogaster. Mol Cell Biol. 2003;23(24):9117–26.

47. Manning BD, Toker A. AKT/PKB signaling: navigating the network. Cell. 2017;169(3):381–405.
48. Soloaga A, Thomson S, Wiggin GR, Rampersaud N, Dyson MH, Hazzalin CA, et al. *MSK2* and *MSK1* mediate the mitogen- and stress-induced phosphorylation of histone H3 and HMG-14. EMBO J. 2003;22(11):2788–97.
49. Zhao QY, Li TX, Song ZJ, Sun T, Liu B, Han X, et al. Combination of modified atmosphere and irradiation for the phytosanitary disinfestation of *Trogoderma granarium* Everts (Coleoptera: Dermestidae). Insects. 2021. https://doi.org/10.3390/insects12050442.
50. Ling DD, Lu SH, Lu YJ, Ren TY, Zheng SZ. Comparison of population development of *Trogoderma granarium* Everts fed by four hosts. Plant Quarantine. 2020;34:9–12.
51. Vurture GW, Sedlazeck FJ, Nattestad M, Underwood CJ, Fang H, Gurtowski J, et al. GenomeScope: fast reference-free genome profiling from short reads. Bioinformatics. 2017;33(14):2202–4.
52. Koren S, Walenz BP, Berlin K, Miller JR, Bergman NH, Phillippy AM. Canu: scalable and accurate long-read assembly via adaptive k-mer weighting and repeat separation. Genome Res. 2017;27(5):722–36.
53. Li H, Durbin R. Fast and accurate short read alignment with Burrows-Wheeler transform. Bioinformatics. 2009;25(14):1754–60.
54. Walker BJ, Abeel T, Shea T, Priest M, Abouelliel A, Sakthikumar S, et al. Pilon: an integrated tool for comprehensive microbial variant detection and genome assembly improvement. PLoS One. 2014;9(11):e112963.
55. Durand NC, Shamim MS, Machol I, Rao SS, Huntley MH, Lander ES, et al. Juicer provides a one-click system for analyzing loop-resolution Hi-C experiments. Cell Syst. 2016;3(1):95–8.
56. Dudchenko O, Batra SS, Omer AD, Nyquist SK, Hoeger M, Durand NC, et al. De novo assembly of the Aedes aegypti genome using Hi-C yields chromosome-length scaffolds. Science. 2017;356(6333):92–5.
57. Durand NC, Robinson JT, Shamim MS, Machol I, Mesirov JP, Lander ES, et al. Juicebox provides a visualization system for Hi-C contact maps with unlimited zoom. Cell Syst. 2016;3(1):99–101.
58. Seppey M, Manni M, Zdobnov EM. BUSCO: assessing genome assembly and annotation completeness. Methods Mol Biol. 2019;1962:227–45.
59. Tang H, Bowers JE, Wang X, Ming R, Alam M, Paterson AH. Synteny and collinearity in plant genomes. Science. 2008;320(5875):486–8.
60. Flynn JM, Hubley R, Goubert C, Rosen J, Clark AG, Feschotte C, et al. RepeatModeler2 for automated genomic discovery of transposable element families. Proc Natl Acad Sci U S A. 2020;117(17):9451–7.
61. Tarailo-Graovac M, Chen N. Using RepeatMasker to identify repetitive elements in genomic sequences. Curr Protoc Bioinformatics. 2009;4:4.10.1-4..4.
62. Leskovec J, Sosic R. SNAP: a general purpose network analysis and graph mining library. ACM Trans Intell Syst Technol. 2016;8(1):1–20.
63. Stanke M, Morgenstern B. AUGUSTUS: a web server for gene prediction in eukaryotes that allows user-defined constraints. Nucleic Acids Res. 2005;33(suppl_2):W465-W7.
64. Haas BJ, Salzberg SL, Zhu W, Pertea M, Allen JE, Orvis J, et al. Automated eukaryotic gene structure annotation using EVidenceModeler and the program to assemble spliced alignments. Genome Biol. 2008;9(1):R7.
65. Buchfink B, Reuter K, Drost H-G. Sensitive protein alignments at tree-of-life scale using DIAMOND. Nat Methods. 2021;18(4):366–8.
66. Gotz S, Garcia-Gomez JM, Terol J, Williams TD, Nagaraj SH, Nueda MJ, et al. High-throughput functional annotation and data mining with the Blast2GO suite. Nucleic Acids Res. 2008;36(10):3420–35.
67. Huerta-Cepas J, Forslund K, Coelho LP, Szklarczyk D, Jensen LJ, von Mering C, et al. Fast genome-wide functional annotation through orthology assignment by eggNOG-mapper. Mol Biol Evol. 2017;34(8):2115–22.
68. Emms DM, Kelly S. OrthoFinder: phylogenetic orthology inference for comparative genomics. Genome Biol. 2019;20(1):238.
69. Stamatakis A. RAxML version 8: a tool for phylogenetic analysis and post-analysis of large phylogenies. Bioinformatics. 2014;30(9):1312–3.
70. Yang Z. PAML 4: phylogenetic analysis by maximum likelihood. Mol Biol Evol. 2007;24(8):1586–91.
71. Hedges SB, Dudley J, Kumar S. TimeTree: a public knowledge-base of divergence times among organisms. Bioinformatics. 2006;22(23):2971–2.
72. Mendes FK, Vanderpool D, Fulton B, Hahn MW. Cafe 5 models variation in evolutionary rates among gene families. Bioinformatics. 2021;36(22–23):5516–8.
73. Laetsch DR, Blaxter ML. Kinfin: software for taxon-aware analysis of clustered protein sequences. G3 (Bethesda). 2017;7(10):3349–57.
74. Vizueta J, Sanchez-Gracia A, Rozas J. Bitacora: a comprehensive tool for the identification and annotation of gene families in genome assemblies. Mol Ecol Resour. 2020;20(5):1445–52.
75. Sinclair BJ, Coello Alvarado LE, Ferguson LV. An invitation to measure insect cold tolerance: methods, approaches, and workflow. J Therm Biol. 2015;53:180–97.
76. Chen S, Zhou Y, Chen Y, Gu J. Fastp: an ultra-fast all-in-one FASTQ preprocessor. Bioinformatics. 2018;34(17):i884–90.
77. Liao Y, Smyth GK, Shi W. Featurecounts: an efficient general purpose program for assigning sequence reads to genomic features. Bioinformatics. 2014;30(7):923–30.
78. Friedlander MR, Mackowiak SD, Li N, Chen W, Rajewsky N. Mirdeep2 accurately identifies known and hundreds of novel microRNA genes in seven animal clades. Nucleic Acids Res. 2012;40(1):37–52.
79. Kruger J, Rehmsmeier M. RNAhybrid: microrna target prediction easy, fast and flexible. Nucleic Acids Res. 2006;34(Web Server issue):W451-4.
80. R Core Team. R: a language and environment for statistical computing. R Foundation for Statistical Computing, Vienna, Austria. 2021. https://ropensci.org/blog/2021/11/16/how-to-cite-r-and-r-packages/.
81. The FlyBase Consortium/Berkeley *Drosophila* Genome Project/Celera Genomics. *Drosophila melanogaster* strain:y; cn bw sp (fruit fly). GenBank https://www.ncbi.nlm.nih.gov/bioproject/PRJNA13812 (2005).
82. Robertson, H. M., Berlocher, S. H., Walden, K. O., Feder, J. L. and Doellman, M. *Rhagoletis pomonella* isolate Grant_MI, whole genome shotgun sequencing project. GenBank https://www.ncbi.nlm.nih.gov/nuccore/1859382258 (2020).
83. Lee, J., Fujimoto, T., Yamaguchi, K., Shigenobu, S., Sahara, K., Toyoda, A., Shimada, T. *Bombyx mori* strain:p50T (domestic silkworm). GenBank https://www.ncbi.nlm.nih.gov/bioproject/PRJDB15448 (2024).
84. Wan, F., Li, F. and Yin, C. *Cydia pomonella* strain Jiuquan, whole genome shotgun sequencing project. GenBank https://www.ncbi.nlm.nih.gov/nuccore/1604220125 (2018).
85. Qu, J., Murali, S. C., Bandaranaike, D., Bellair, M., Blankenburg, K., Chao, H., Dinh, H., Doddapaneni, H., Downs, B., Dugan-Rocha, S., Elkadiri, S., Gnanaolivu, R. D., Hernandez, B., Javaid, M., Jayaseelan, J. C., Lee, S., Li, M., Ming, W., Munidasa, M., Muniz, J., Nguyen, L., Ongeri, F., Osuji, N., Pu, L.-L., Puazo, M., Qu, C., Quiroz, J., Raj, R., Weissenberger, G., Xin, Y., Zou, X., Richards, S., Han, Y., Worley, K., Muzny, D. and Gibbs, R. *Agrilus planipennis* isolate EAB-ADULT, whole genome shotgun sequencing project. GenBank https://www.ncbi.nlm.nih.gov/nuccore/1318834518 (2014).
86. Cunningham, C. B., Shelton, J. M., Mckinney, E. C., Meagher, R. B., Brown, S. B. and Moore, A. J. *Nicrophorus vespilloides* isolate i.1.1–1, whole genome shotgun sequencing project. GenBank https://www.ncbi.nlm.nih.gov/nuccore/LJCH00000000.1 (2015).
87. Chen, M., Mei, Y., Chen, X., Chen, X., Xiao, D., Wang, S., Zhang, F. and Li, F. *Harmonia axyridis* isolate ZJU_2019, whole genome shotgun sequencing project. GenBank https://www.ncbi.nlm.nih.gov/nuccore/WMPA00000000.2/ (2021).
88. Wellcome Sanger Tree of Life Programme. *Aphidecta obliterata*, whole genome shotgun sequencing project. GenBank https://www.ncbi.nlm.nih.gov/nuccore/2674094126 (2024).
89. Chellapilla, S., Park, Y., Shippy, T., Lu, N., Tank, G. and Brown, S. *Tribolium madens* breed KSU strain isolate multiple individuals, whole genome shotgun sequencing project. GenBank https://www.ncbi.nlm.nih.gov/nuccore/1930350852 (2020).
90. Shelton, J. M., Herndon, N., Coleman, C., Lu, N. and Brown, S. J. *Tribolium castaneum* strain Georgia GA2, whole genome shotgun sequencing project. GenBank https://www.ncbi.nlm.nih.gov/nuccore/1002988972 (2008).
91. Hong, W. *Oryzaephilus surinamensis* isolate S25–3, whole genome shotgun sequencing project. GenBank https://www.ncbi.nlm.nih.gov/nuccore/1616362094 (2017).
92. Qu, J., Richards, S., Bandaranaike, D., Bellair, M., Blankenburg, K., Chao, H., Dinh, H., Doddapaneni, H., Downs, B., Dugan-Rocha, S., Elkadiri, S., Hernandez, B., Javaid, M., Jayaseelan, J. C., Lee, S., Li, M., Ming, W., Munidasa, M., Muniz, J., Nguyen, L., Ongeri, F., Osuji, N., Pu, L.-L., Puazo, M., Qu, C., Quiroz, J., Raj, R., Weissenberger, G., Xin, Y., Zou, X., Han, Y., Worley, K., Muzny, D. and Gibbs, R. *Anoplophora glabripennis* isolate ALB-LARVAE,

whole genome shotgun sequencing project. GenBank https://www.ncbi.nlm.nih.gov/nuccore/1305463464 (2013).
93. Shin, N. R., Okamura, Y., Kirsch, R. and Pauchet, Y. *Exocentrus adspersus* isolate EAD_L_NR, whole genome shotgun sequencing project. GenBank https://www.ncbi.nlm.nih.gov/nuccore/JANEYG000000000.1 (2023).
94. Qu, J., Richards, S., Bandaranaike, D., Bellair, M., Blankenburg, K., Chao, H., Dinh, H., Doddapaneni, H., Downs, B., Dugan-Rocha, S., Elkadiri, S., Hernandez, B., Javaid, M., Jayaseelan, J. C., Lee, S., Li, M., Ming, W., Munidasa, M., Muniz, J., Nguyen, L., Ongeri, F., Osuji, N., Pu, L.-L., Puazo, M., Qu, C., Quiroz, J., Raj, R., Weissenberger, G., Xin, Y., Zou, X., Han, Y., Worley, K., Muzny, D. and Gibbs, R. *Leptinotarsa decemlineata* strain imidocloprid resistant, whole genome shotgun sequencing project. GenBank https://www.ncbi.nlm.nih.gov/nuccore/1272951028 (2013).
95. Wellcome Sanger Tree of Life Programme. *Bruchidius siliquastri*, whole genome shotgun sequencing project. GenBank https://www.ncbi.nlm.nih.gov/nuccore/2453100199 (2023).
96. Wellcome Sanger Tree of Life Programme. *Platypus cylindrus*, whole genome shotgun sequencing project. GenBank https://www.ncbi.nlm.nih.gov/nuccore/2478403133 (2023).
97. Keeling, C. I., Yuen, M., Liao, N. Y., Docking, R. T., Chan, S. K., Taylor, G. A., Palmquist, D. L., Jackman, S. D., Nguyen, A., Li, M., Henderson, H., Janes, J. K., Zhao, Y., Pandoh, P., Moore, R., Sperling, F. A. H., Huber, D. P. W., Birol, I., Jones, S. J. M. and Bohlmann, J. *Dendroctonus ponderosae*, whole genome shotgun sequencing project. GenBank https://www.ncbi.nlm.nih.gov/nuccore/462478414 (2013).

## Publisher's Note